Contribution from the Chemistry Departments, Polytechnic Institute of Brooklyn, Brooklyn, New York 11201, and University of Wyoming, Laramie, Wyoming 82070

Crystal Spectrum of Bis(salicylidene-γ-iminopropyl)aminonickel(II) and Bis(salicylidene-γ-iminopropyl)methylaminonickel(II)

M. NEMIROFF* and S. L. HOLT

Received March 16, 1972

The electronic symmetries of the two similar five-coordinate compounds bis(salicylidene-γ-iminopropyl)aminonickel(II) (Ni(saldipa)) and bis(salicylidene-γ-iminopropyl)methylaminonickel(II) (Ni(salmedpt)) were found to differ. The ligand geometry about nickel is very similar for both compounds. The effective electronic symmetry about Ni(saldipa) best fits D_{3h} symmetry. However, the temperature dependence of at least two of the absorption bands in Ni(salmedpt) indicate that the effective electronic symmetry of this compound is C_{2v}.

Introduction

Single-crystal spectral techniques have found wide use in recent times to help elucidate problems relating to the electronic structure of transition metal ions. As a rule however these techniques have been confined to compounds in which the coordination around the central ion is four or six. Part of this arises from the fact that the structural work available for reference has been heavily concentrated in these areas. Present circumstances have altered this picture however and we now have available to us a number of complete structures of five-coordinate compounds. We have chosen to investigate two of these which are chemically and physically similar: bis(salicylidene-γ-iminopropyl)aminonickel(II), Ni(saldipa), and bis(salicylidene-γ-iminopropyl)methylaminonickel(II), Ni(salmedpt)

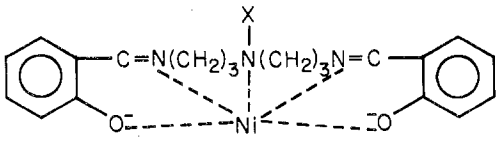

Ni(saldipa), X = H
Ni(salmedpt), X = CH_3

Experimental Section

Both Ni(saldipa) and Ni(salmedpt) were synthesized by the method of Sacconi.[1] The measurement of electronic spectra required large thin plates for the maximum transmission of light since both pure compounds have a high density of absorbing centers. The largest and thinnest diamond-shaped plates of Ni(saldipa) were grown from a 80:20 mixture of methylene chloride and acetone. Crystals with which the final data were taken were plates of dimensions 4 × 3 × 0.2 mm. These crystals were mounted on a brass ring and placed in the optical well of a helium dewar. The polarized spectra were taken at liquid helium temperature with $\vec{E} \| b$ and c axes using techniques previously described.[2-5] See Figure 1.

The best plates of Ni(salmedpt) were grown from acetone. These developed as prisms with a large rectangular face but were too thick and had to be polished with acetone in order to ensure sufficient light transmission. The crystals used for the final data collection typically had dimensions of 5 × 3 × 0.2 mm. Data were collected with $\vec{E} \| a$ and $\vec{E} \| b$. See Figure 2.

Crystal Structures

The structure of Ni(saldipa) has been determined by Seleborg, *et al.*[6] The projection of the contents of the unit cell along the a axis, eliminating all atoms except the five nearest neighbors to the nickel atom, is shown in Figure 1. The structure of Ni(salmedpt) has been reported by Di Vaira, *et al.*[7] A projection of the contents of the unit cell along the c axis, eliminating all but the five nearest nickel neighbors is shown in Figure 2. Both molecules have very similar molecular geometries which can be approximated as distorted trigonal bipyramids (TBP). This requires that the molecular z axis be defined by the atoms N(3), Ni, and N(2) and the x,y plane be defined by the atoms N(1), O(1), and O(2).

For these molecules to have a TBP configuration the N(3)-Ni-N(2) angle should be 180°, the angle between the z axis and the x,y plane should be 90°, and the ligand-Ni-ligand angles in the x,y plane should all be 120°. As may be seen in Table I, the z axis-equatorial plane deviations are small. The equatorial-equatorial deviations are large however. The large distortion from trigonal symmetry in the equatorial plane might be sufficient to cause splitting of all orbital degeneracies, lowering the electronic as well as the molecular symmetry to C_{2v} or C_2.

Results

The spectrum of Ni(salmedpt) taken at 300 and at 80°K with $\vec{E} \| a$ is shown in Figure 3. The energies of the important maxima which occur in this spectrum are tabulated in Table II. Note should be taken of the fact that maxima shift ~300 cm^{-1} toward the blue end of the spectrum upon cooling the sample to 80°K but the integrated intensity is fairly constant.

The spectrum with $\vec{E} \| b$ is shown in Figure 4. As with the first spectrum a moderate shift toward the blue with decreasing temperature is observed. In addition, however, two maxima, those at 8500 and 17,300 cm^{-1}, show a marked intensity *vs.* temperature dependence. The spectrum of Ni(saldipa) taken at 300 and 80°K with $\vec{E} \| c$ is shown in Figure 5. The spectrum taken with $\vec{E} \| b$ is shown in Figure 6. The spectrum taken at 5°K is shown in Figure 7.

The location of the maxima and the shift toward the blue at low temperatures are quite similar to those of Ni(salmedpt); however, there is no apparent temperature dependence in the Ni(saldipa) spectrum. The appropriate energy maxima of Ni(saldipa) are reported in Table II.

Discussion

Ciampolini[8] has calculated crystal field diagrams for five-coordinated trigonal-bipyramidal and square-pyramidal ligand fields about Ni(II). Crystal field diagrams for both these

* To whom correspondence should be addressed at the Polytechnic Institute of Brooklyn.

(1) L. Sacconi, P. L. Orioli, and M. Di Vaira, *J. Amer. Chem. Soc.*, 87, 2059 (1965).
(2) C. Simo and S. L. Holt, *Inorg. Chem.*, 7, 2655 (1968).
(3) E. Banks, M. Greenblatt, and S. L. Holt, *J. Chem. Phys.*, 49, 1431 (1968).
(4) J. Milstein and S. L. Holt, *Inorg. Chem.*, 8, 1021 (1969).
(5) C. Simo, E. Banks, and S. L. Holt, *Inorg. Chem.*, 8, 1446 (1969).
(6) M. Seleborg, S. L. Holt, and B. Post, *Inorg. Chem.*, 10, 1501 (1971).
(7) M. Di Vaira, P. L. Orioli, and L. Sacconi, *Inorg. Chem.*, 10, 553 (1971).
(8) M. Ciampolini, *Inorg. Chem.*, 5, 35 (1966).

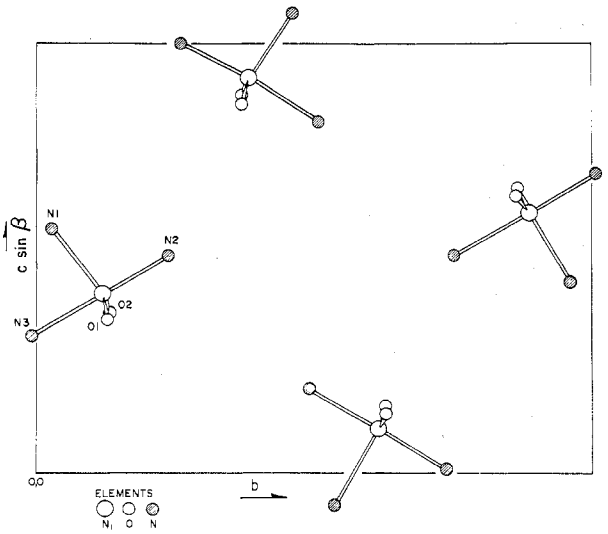

Figure 1. Projection of the NiN_3O_2 moiety in Ni(saldipa) along *a*.

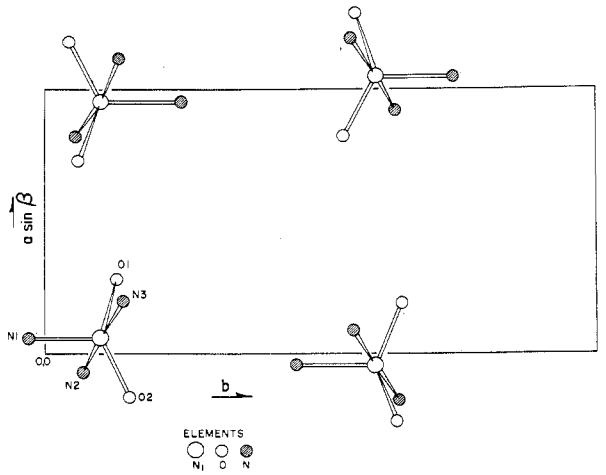

Figure 2. Projection of the NiN_3O_2 moiety in Ni(salmedpt) along *c*.

Table I. Bond Angles (deg) about Nickel for the Five-Coordinate Compounds Ni(saldipa) and Ni(salmedpt)

Angle	Ni(saldipa)	Ni(salmedpt)
N(3)-Ni-O(1)	90.7 (2)	89.8 (3)
O(1)-Ni-O(2)	145.7 (2)	140.6 (3)
O(2)-Ni-N(3)	93.4 (2)	89.9 (3)
N(3)-Ni-N(2)	177.2 (2)	177.0 (3)
N(3)-Ni-N(1)	91.5 (3)	91.1 (3)
O(1)-Ni-N(2)	86.7 (2)	88.8 (3)
O(1)-Ni-N(1)	111.4 (2)	113.5 (3)
O(2)-Ni-N(2)	88.3 (2)	89.5 (3)
O(2)-Ni-N(1)	102.5 (2)	105.9 (3)
N(2)-Ni-N(1)	90.1 (2)	91.8 (3)

Table II. Energies (cm^{-1}) of Important Absorption Maxima in the Electronic Spectra of Ni(salmedpt) and Ni(saldipa) (at 80°K)[a]

Ni(salmedpt)		Ni(saldipa)	
$\vec{E}\|\|a$	$\vec{E}\|\|b$	$\vec{E}\|\|b$	$\vec{E}\|\|c$
8,700 w	8,600 m	7,800 w, sp	8,900 m
10,100 m	10,000 s	8,900 s	10,700 m
11,600 w	11,800 w	10,800 sh	11,700 w, sh
13,900 sh	13,100 sh	11,700 w, sp	14,000 m-w
17,300 s	13,900 m	14,200 m-w, b	17,300 m-s
	17,300 s	17,300 s	21,300 sh, s
		21,300 sh, s	

[a] Key: b, broad; m, medium; s, strong; sh, shoulder; sp, sharp; w, weak.

types of orientation with $\beta = 90°$ for the square-pyramidal (SP) case are shown in Figure 8. β is the angle L_{ax}-Ni-L_{base} where L_{ax} = axial ligand(s) and L_{base} = any of the basal ligands. Ciampolini[8] has found that solution spectra of some five-coordinated compounds fit his data for known SP and trigonal-bipyramidal (TBP) structures where $\mu = 5.0$. μ is the point dipole strength of the ligands. If $\mu = 5.0$ and the geometry is TBP (D_{3h}) spin-allowed transitions should occur at 7000, 14,000, 15,000, 22,000, and 26,000 cm^{-1}. Spin-forbidden transitions should occur at 7000, 14,000, and 19,000 cm^{-1}. If the geometry is SP (C_{4v}), spin-allowed transitions should occur at 9000, 11,000, 13,000, and 20,000 cm^{-1}. Spin-forbidden transitions should occur at 7000, 19,000, 21,000, and 22,000 cm^{-1}.

Spin-Allowed Transitions in Ni(saldipa). The spectrum of Ni(saldipa) at ambient room and liquid nitrogen temperatures showed no significant difference in oscillator strength of the spin-allowed bands. Therefore, none of the observed transitions in Figure 5 or 6 are allowed *via* vibronic mechanism. In these spectra the spin-allowed bands appear at 8900, 10,800, 13,990, 17,300, and 21,300 cm^{-1} before the onset of the charge-transfer band. What appear to be two spin-forbidden bands occur at 7800 and 11,700 cm^{-1}.

The triplet-triplet transitions for TBP and SP geometry are presented in order of their increasing energy in accordance with their predicted polarization behavior in Table III. The Ni(saldipa) NiN_3O_2 moiety projected perpendicular to the *a* axis is shown in Figure 1. In TBP geometry the atoms N(2), Ni, and N(3) form the *x,y* plane. In SP geometry the N(1)-Ni bond is the *z* molecular axis and the atoms N(2), N(3), O(1), and O(2) form the *x,y* plane. This is also the case for Ni(salmedpt) in Figure 2.

If the effective electronic symmetry is SP (Table IV), then the lowest and highest energy transitions are allowed with $\vec{E}\|x,y$. Therefore these transitions should be stronger with $\vec{E}\|b$ than $\vec{E}\|c$. This is what is observed. However, the second and third energy bands are forbidden and should show temperature dependence. This is not the case. The fifth and highest energy transition observed should be forbidden. Intensity can be observed only through a vibronic mechanism. This is not the case since the band is resolved at 80°K.

If the effective electronic symmetry is TBP (Table III), then the first and fourth bands (8900 and 17,300 cm^{-1}) are allowed with $\vec{E}\|z$ and should be more intense with $\vec{E}\|b$ than with $\vec{E}\|c$. This is also the case in C_{4v} symmetry. In TBP symmetry the second, third, and fifth bands (10,800, 13,990, and 21,300 cm^{-1}) are allowed with $\vec{E}\|x,y$ and should be more strongly polarized with $\vec{E}\|c$ than $\vec{E}\|b$. The second band appears as a shoulder on the first band in *b* polarization (Figure 7). Because of this the polarization of this band cannot be assigned. The third band does appear polarized with $\vec{E}\|c$. The fifth band appears as a shoulder on the intense charge-transfer band. Its polarization also cannot be assigned.

The true symmetry of Ni(saldipa) is quite close to C_{2v}, with Ni-N(1) forming the molecular *z* axis. Since this compound does exhibit polarization, the electronic symmetry cannot be C_1. A correlation table and correlations for allowed transitions for $D_{3h} \rightarrow C_{2v} \rightarrow C_2$ are presented in Table III. In both C_{2v} and C_2 symmetries the degeneracy of the E states is split; however, the energy differences of these states might be too small to be resolved. If the true symmetry of Ni(saldipa) is C_{2v}, then the spectra should exhibit temperature dependence since transitions to one member of each pair of the first, second, and fourth transitions are forbidden. This is not the case and rules out C_{2v} as a possible choice. If the electronic symmetry is C_2, then the first band to exhibit polarized behavior would be the third band. This band and the fifth

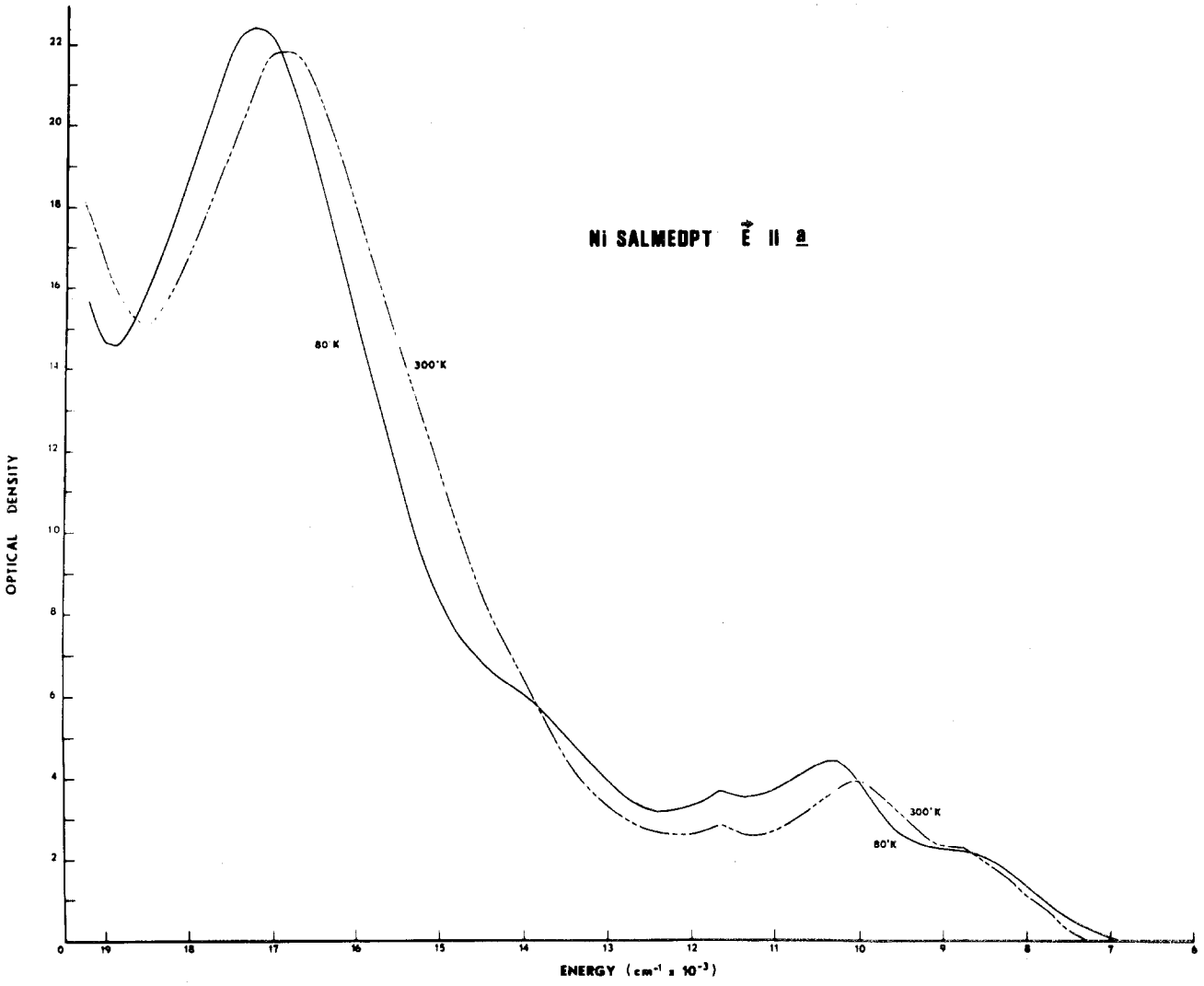

Figure 3. Spectrum of Ni(salmedpt) with $\vec{E} \| a$ at 80 and 300°K.

Table III. Allowed Transitions $C_{4v}, D_{3h} \rightarrow C_{2v} \rightarrow C_2$

		C_{2v}		C_2	
$C_{4v}, \beta = 90°$	D_{3h}	$^3B_2$ ground state	$^3A_1$ ground state	^3A ground state	^3B ground state
$^3B_1 \rightarrow {}^3E \| x,y$	$^3E' \rightarrow {}^3E'' \| z$	$^3B_2 \rightarrow {}^3A_2 \| x$	$^3A_1 \rightarrow {}^3A_2$ forbidden	$^3A \rightarrow {}^3A \| z$	$^3B \rightarrow {}^3A \| x,y$
		$\rightarrow {}^3B_1$ forbidden	$\rightarrow {}^3B_1 \| x$	$\rightarrow {}^3B \| x,y$	$\rightarrow {}^3B \| z$
$^3B_1 \rightarrow {}^3A_2$ forbidden	$\rightarrow {}^3A_2'', {}^3A_1'' \| x,y$	$\rightarrow {}^3B_2 \| x$	$\rightarrow {}^3A_2$ forbidden	$\rightarrow {}^3A \| z$	$\rightarrow {}^3A \| x,y$
		$\rightarrow {}^3B_1$ forbidden	$\rightarrow {}^3B_1 \| x$	$\rightarrow {}^3A \| x,y$	$\rightarrow {}^3B \| z$
$^3B_1 \rightarrow {}^3B_2$ forbidden	$\rightarrow {}^3A_2' \| x,y$	$\rightarrow {}^3B_2 \| z$	$\rightarrow {}^3B_2 \| y$	$\rightarrow {}^3B \| x,y$	$\rightarrow {}^3B \| z$
$^3B_1 \rightarrow {}^3E \| x,y$	$\rightarrow {}^3E'' \| z$	$\rightarrow {}^3A_2 \| x$	$\rightarrow {}^3A_2$ forbidden	$\rightarrow {}^3A \| z$	$\rightarrow {}^3A \| x,y$
		$\rightarrow {}^3B_1$ forbidden	$\rightarrow {}^3B_1 \| y$	$\rightarrow {}^3B \| x,y$	$\rightarrow {}^3B \| z$
$^3B_1 \rightarrow {}^3A_2$ forbidden	$\rightarrow {}^3A_2' \| x,y$	$\rightarrow {}^3B_2 \| z$	$\rightarrow {}^3B_2 \| y$	$\rightarrow {}^3B \| x,y$	$\rightarrow {}^3B \| z$
$^3B_1 \rightarrow {}^3E \| x,y$					

Table IV. Correlation Table for $D_{3h} \rightarrow D_3'$

D_{3h}	$\rightarrow$	D_3	$\rightarrow$	D_3'
$^1A_1'$		$^1A_1$		Γ_1
$^1E'$		^1E		Γ_3
$^1E''$		^1E		Γ_3

band would exhibit similar polarizations. The other three bands would show no polarization. This would require considerable shifting of the transition energies and excludes C_2 as the effective electronic symmetry. In addition, the fact that the spectrum of Ni(saldipa) is not temperature dependent excludes C_{4v} as a possible choice.

Although there are large distortions from TBP symmetry in the trigonal plane of the Ni(saldipa) the polarization behavior indicates that the effective electronic symmetry best fits TBP. The ordering of the energy of the d orbitals in this environment from highest to lowest is $d_{z^2} = a' > d_{x^2-y^2}$, $d_{xy} = e' > d_{xz}, d_{yz} = e''$. The ground state is then $e''^4 e'^3 a_1'^1$.

The first four spin-allowed transitions for a TBP arrangement of ligands about Ni(II), when $\mu = 5.0$, should occur at 7000, 14,000, 15,000, and 22,000 cm^{-1}. The spectrum of Ni(saldipa) at liquid He with $\vec{E} \| b$ exhibits maxima at 8900, 10,800, 13,990, and 17,300 cm^{-1}. Since the second and third bands exhibit similar polarization behaviors and lie so close together in Ciampolini's diagram[8] for $\mu = 5.0$, the choice of assignments for the second and third transitions is not clear. The assignments for the five spin-allowed transitions in Ni(saldipa) are $^3E' \rightarrow {}^3E''$ (8900 cm^{-1}), $^3A_2'$ or $^3A_1''$, $^3A_2''$ (10,800 cm^{-1}), $^3A_2'$ or $^3A_1''$, $^3A_2''$ (13,900 cm^{-1}), $^3E''$ (17,300 cm^{-1}), and $^3A_2'$ (21,300 cm^{-1}).

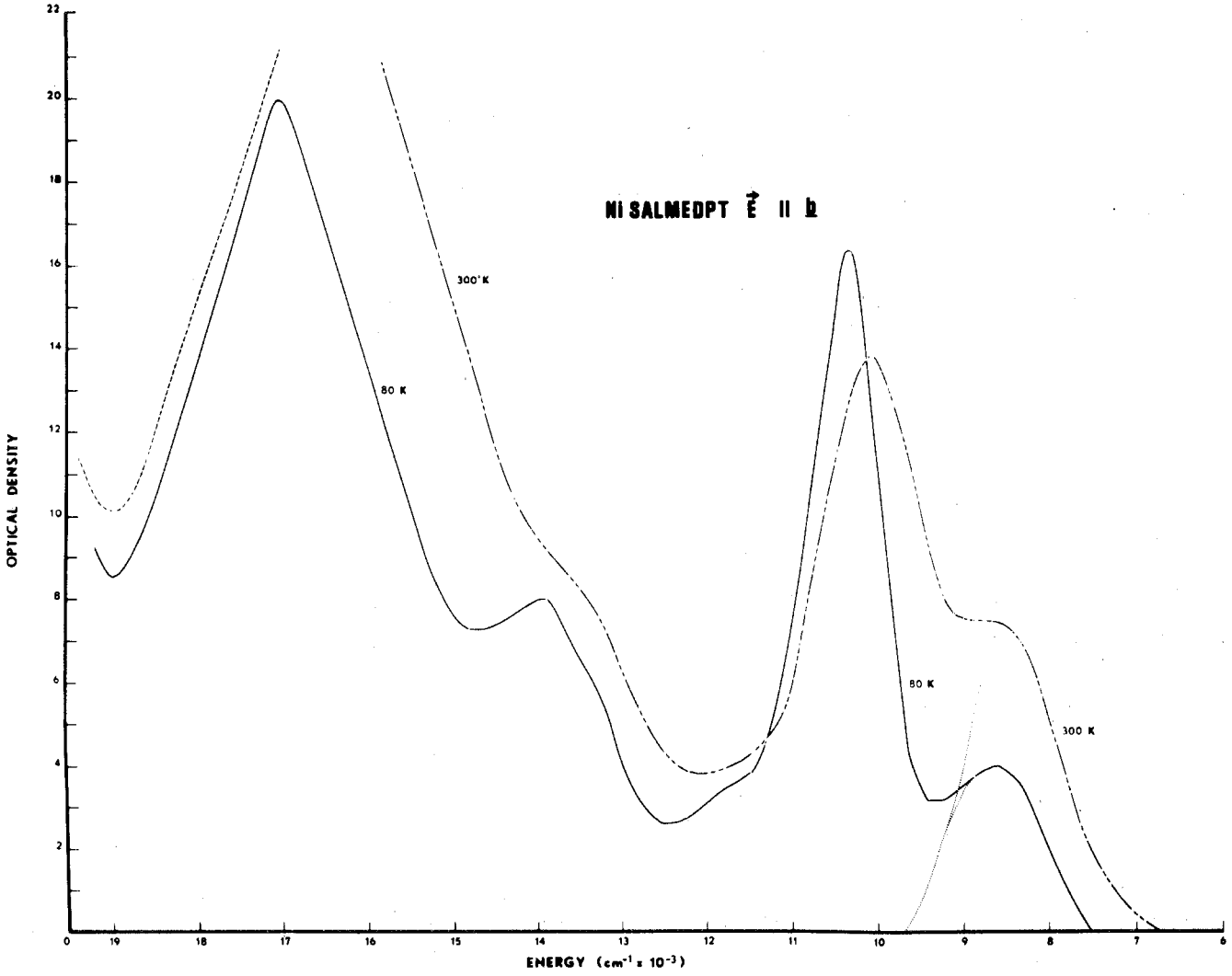

Figure 4. Spectrum of Ni(salmedpt) with $\vec{E} \| b$ at 80 and 300°K.

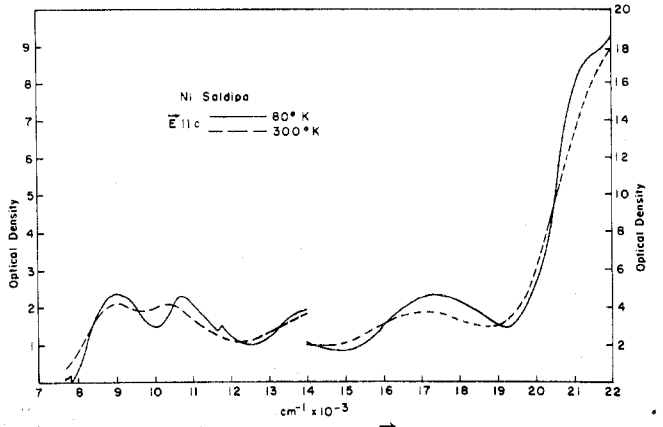

Figure 5. Spectrum of Ni(saldipa) with $\vec{E} \| c$ at 80 and 300°K.

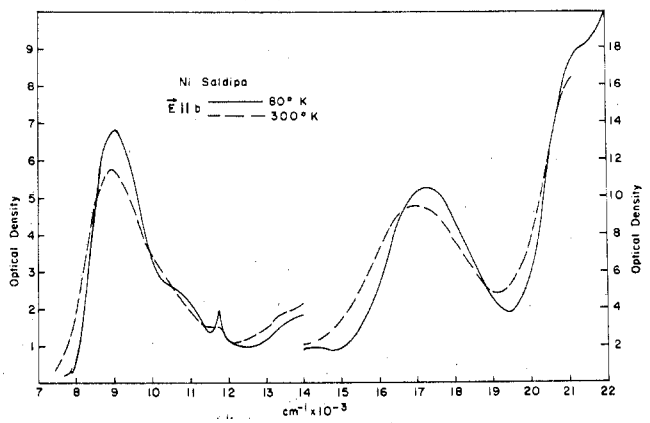

Figure 6. Spectrum of Ni(saldipa) with $\vec{E} \| b$ at 80 and 300°K.

Transitions to Singlet States in Ni(saldipa). In TBP symmetry three transitions to singlet states, *i.e.*, $^3E' \rightarrow {}^1A_1'$, $^1E'$, and $^1E''$, are predicted below 20,000 cm^{-1} before the onset of the charge-transfer band. Two of them, one at 7900 cm^{-1} and the other at 11,800 cm^{-1}, appear in the Ni(saldipa) spectrum with $\vec{E} \| b$. The transition at 11,800 cm^{-1} also occurs as a weak shoulder in the spectrum with $\vec{E} \| c$.

In accounting for these peaks we note that the singlet $s = 0$ state transforms as Γ_1 and the triplet state $s = 1$ transforms as $\Gamma_2 + \Gamma_3$ in the D_3' double group. The correlation for $D_{3h} \rightarrow D_3'$ is given in Table IV. The transitions $^3E \rightarrow {}^1A$ and $^3E \rightarrow {}^1E$ both yield the representations Γ_1, Γ_2, and Γ_3. Since x,y transforms as E (Γ_3) and z transforms as A_2 (Γ_2) and since the spin-allowed excited states transform as either (Γ_1, Γ_2, Γ_3) ^3E, (Γ_3) $^3A_1$, or (Γ_3) $^3A_2$, then all these transitions are very weakly allowed. That only two of the spin-forbidden transitions appear in Ni(saldipa) might be due to the fact that the missing energy transition at 19,000 cm^{-1} is under the charge-transfer band or under the spin-allowed transition at 17,300 cm^{-1} if the true energy of the spin-forbidden band is lowered by a few thousand wave numbers.

Since these singlet transitions can borrow intensity from

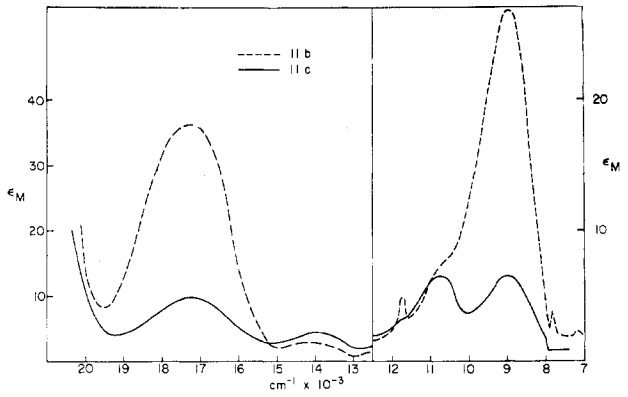

Figure 7. Spectrum of Ni(saldipa) at 5°K with $\vec{E}\|b$ and $\vec{E}\|c$.

the "allowed" transitions, the stronger bands in *b* polarization (Figure 5) can be accounted for simply because the two strong bands at 8900 and 17,300 cm^{-1} are more strongly polarized along the *b* axis.

The singlet transitions then can be classified as $^3E \rightarrow {}^1A_1'$ (7800 cm^{-1}) and $^1E'$ (11,700 cm^{-1}). However, since these selection rules are not so powerful, the effective electronic symmetry is more strongly determined by the allowed transitions.

Spin-Allowed Transitions in Ni(salmedpt). The spectrum of Ni(salmedpt) with $\vec{E}\|a$ is shown in Figure 3; that with $\vec{E}\|b$ is shown in Figure 4. Although the positions of the bands are quite similar to those in Ni(saldipa), the polarization behavior is not. This can be partly attributed to differences in the orientation of the molecular axes with respect to the crystal axes. For example, in Figure 2, if the atoms N(2), Ni, and N(3) form the *z* molecular axis in TBP symmetry and N(1), O(1), O(2), and Ni form the trigonal *xy* plane, then the *x*, *y*, and *z* axes are quite displaced relative to the crystal axes. This is not true in Ni(saldipa) where the *z* axis is nearly in the *bc* plane. However, a feature of the spectrum of Ni(salmedpt) which is not attributable to the misalignment of the molecular axes with respect to the crystal axes is the temperature dependence of the bands at 8500 and 17,300 cm^{-1} with $\vec{E}\|b$. Clearly these bands are vibronically allowed. This does not fit D_{3h} symmetry since the first four bands are allowed with $\vec{E}\|$ to either *z* or *x*,*y* as shown in Table III. In C_{4v} symmetry the middle two bands are vibronically allowed. However, it is unlikely that there has been such a shift of the bands. In addition, the transition $^3B_1 \rightarrow {}^3B_2$ is vibronically allowed with $\vec{E}\|x,y$ only. The selection rules imply that this band should be more strongly polarized with $\vec{E}\|a$, since O(1), O(2), N(2), and N(3) form the *xy* plane in C_{4v} symmetry. This is not the case. The polarization is stronger with $\vec{E}\|b$. For these reasons C_{4v} is also not a suitable model for the effective electronic symmetry of Ni(salmedpt). The actual geometrical symmetry of Ni(salmedpt) is C_1. However, the symmetry is also quite close to C_{2v} with the Ni–N(1) bond forming the *z* axis. The atoms O(2), Ni, and O(1) form the *yz* plane and the atoms N(2), Ni, and N(3) form the *xz* plane.

As can be seen from Table III, three sets of bands contain one allowed and one forbidden transition from the nondegenerate pair A_2, B_1 in C_{2v} symmetry. One of the transitions is allowed with $\vec{E}\|x$. This would account for the polarization behavior of Ni(salmedpt). For even though the three bands contain a nondegenerate pair, the differences in energy between transitions to both members of the pair are most likely too small to be resolved. The forbidden transition of each pair would then gain intensity through a vibronic mechanism. The choice of ground state $^3A_1$ or $^3B_2$ is dictated by the polarization of transition to the $^3B_2$ state. If the ground state is $^3A_1$, the transition $^3A_1 \rightarrow {}^3B_2$ is allowed with $\vec{E}\|y$. If the ground state is $^3B_2$, the transition $^3B_2 \rightarrow {}^3B_2$ is allowed with $\vec{E}\|z$. The transition at 10,300 cm^{-1} is the only one which is clearly not temperature dependent. It shows *b*

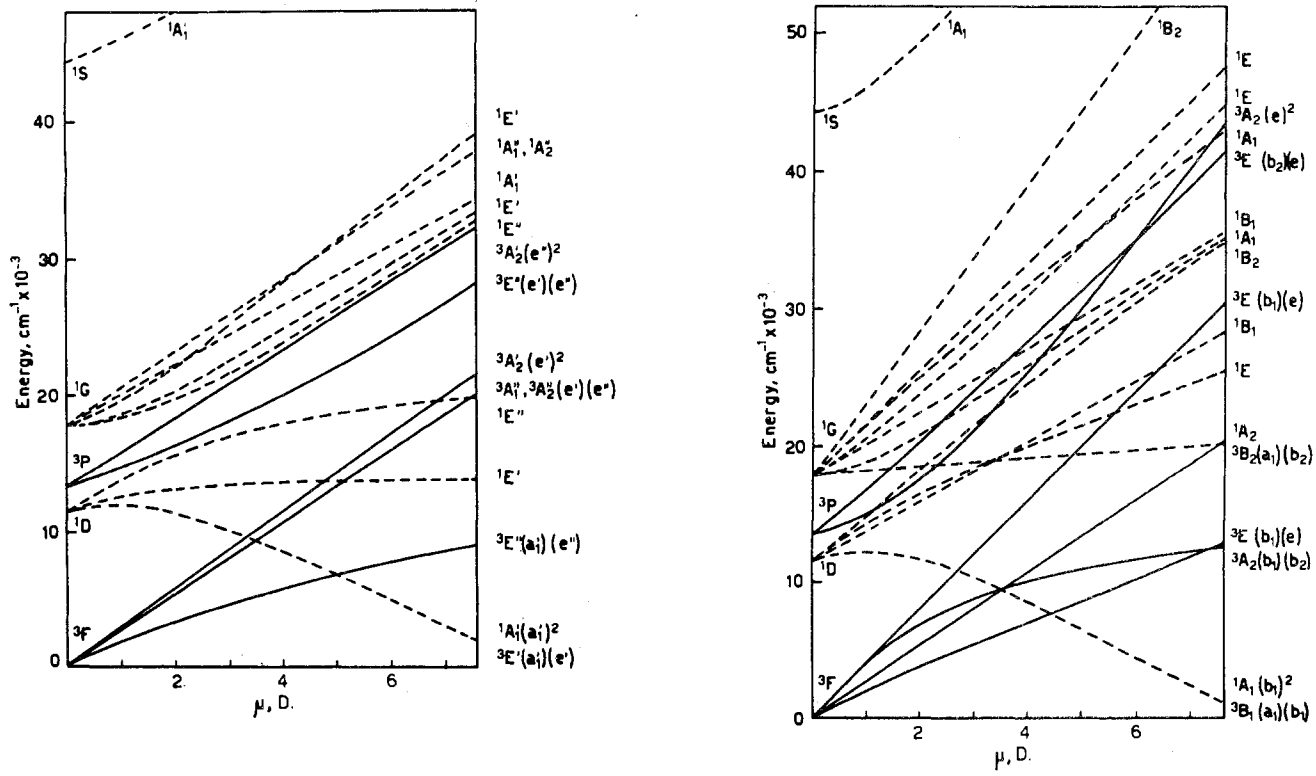

Figure 8. Crystal field diagrams for five-coordinate Ni(II): (left) for a trigonal-bipyramidal arrangement of five equivalent dipoles; (right) for a square-pyramidal arrangement of five equivalent dipoles with $L_{ax}NiL_{base} = 90°$.

polarization. This transition is $^3B_2 \rightarrow {}^3B_2$, because of its b ($\vec{E} \| z$) polarization. This then reverses the order of the *middle two* transitions. The other two transitions are assigned as $^3B_2 \rightarrow {}^3A_2$, $^3B_1$.

The spin-allowed transitions in Ni(salmedpt) are $^3B_2 \rightarrow {}^3A_2$, $^3B_1$ (8600 cm^{-1}), $^3B_2$ (10,000 cm^{-1}), $^3A_2$, $^3B_1$ (13,960 cm^{-1}), and $^3A_2$, $^3B_1$ (17,300 cm^{-1}).

Spin-Forbidden Transitions in Ni(salmedpt). Two transitions which can be classified as spin forbidden occur at 11,800 and 13,300 cm^{-1}. The 11,800-cm^{-1} band also occurs in the spectrum of Ni(saldipa). The band at 13,300 cm^{-1} may be related to a band which lies under an allowed transition in Ni(saldipa). If the true electronic symmetry is C_{2v}, then transitions to singlet states should obey selection rules based on the double group C_2'. The correlation for $C_{2v} \rightarrow C_2'$ is given in Table V. The singlet transitions are $^3B_2 \rightarrow {}^1A_1$, $^1A_1 + {}^1B_2$, and $^1A_2 + {}^1B_1$. The direct product of the ground state and the first singlet excited state transforms as Γ_2. The direct product of the ground state and the second and third excited states transforms as $\Gamma_1 + \Gamma_2$. All allowed transitions will couple with these irreducible representations to produce transitions which are very weakly allowed parallel to either z or x,y. All transitions to singlet states are then very weakly allowed and the relative intensity of these transitions would be expected to be slightly stronger with $\vec{E} \| b$ than with $\vec{E} \| a$ since the allowed bands in the near-infrared region are stronger in b polarization.

Conclusion

The effective electronic symmetries about the Ni(saldipa) are different. Ni(saldipa) best fits D_{3h} symmetry and Ni(salmedpt) exhibits C_{2v} symmetry. This is surprising in view of the very similar geometry of the five atoms closely coordinated to nickel in both cases. However, the polarization data demand this type of interpretation. There are two possible interpretations for this difference in electronic symmetry. It is possible that either the differences in bond angles or the fact that N(1) is secondary in Ni(saldipa) and tertiary in Ni(salmedpt) could cause a difference in effective electronic symmetry. The angular differences are small: the largest is 5° for O(1)-Ni-O(2). The fact that transitions in Ni(saldipa) can be assigned on the basis of D_{3h} symmetry where the O(1)-Ni-O(2) angle is 25° larger than the ideal trigonal angle rules out the first possibility. Therefore we must conclude that the bonding about nitrogen strongly influences the effective electronic symmetry in these compounds.

Table V. Correlation Table for $C_{2v} \rightarrow C_2'$

C_{2v}	→	C_2	→	C_2'
A_1		A		Γ_1
A_2		A		Γ_1
B_1		B		Γ_2
B_2		B		Γ_2

Registry No. Ni(saldipa), 40685-46-9; Ni(salmedpt), 40754-29-8.

Acknowledgment. We wish to thank Professor Ciampolini for permission to reprint his crystal field diagrams and the National Science Foundation which supported this work in part through Grant GP 15432.

Contribution from Department of Chemistry,
North Carolina State University, Raleigh, North Carolina 27607

Magnetic Circular Dichroism, Crystal Field, and Related Studies of Nickel(II) Amines

A. F. SCHREINER* and D. J. HAMM

Received August 8, 1972

Complexes $[Ni(NH_3)_6]A_2$ ($A = ClO_4^-$, Cl^-), *trans*-$[Ni(py)_4L_2]Q$ ($L = NCO^-$, NCS^-, $NCSe^-$, N_3^-, py), and *trans*-$[Ni(py)_4X_2]$ ($X = Cl^-$, Br^-, I^-) have been examined by obtaining variously MCD, low-temperature electronic, and laser Raman data, crystal field parameters from the rapid Newton-Raphson solution-seeking method, and single-crystal X-ray data. New vibronic fine structure was observed and band assignments were made, and MCD parameters from moment analysis and gaussian decompositions were compared. Overall the MCD data can be understood by the recently proposed model of Harding, Mason, Robbins, and Thomson for $[Ni(NH_3)_6]^{2+}$. Finally, it was found that the single-crystal X-ray diffraction data for $[Ni(py)_4I_2]$ gave orthorhombic space group $D_{2h}{}^{14}$, $Z = 4$, and cell dimensions 9.678, 16.076, and 14.004 Å for a, b, and c. The planes of the pyridine rings were found to make an approximate angle of 45° with the (NiN_4) plane of the coordination sphere, similar to the *assumed* angle of the previously studied Cl^- and Br^- complexes. The two average nickel-ligand atom distances are 2.11 and 2.88 Å for Ni–N and Ni–I, respectively.

Introduction

Having the interest of characterizing properties of electronic excited states, we are particularly interested in determining what contributions the magnetic circular dichroism (MCD) technique can make toward achieving that goal. The method appeared especially suitable for the six-coordinate Ni(II) molecules of interest here (O_h and D_{4h}), since Faraday A parameters should in principle be extractable for orbital $T(O_h)$ and $E(D_{4h})$ states, and these parameters would also characterize such states[1] and in principle immediately distinguish them from nondegenerate orbital states. While the required interpretations turned out to be more complex,[2,3] the MCD data permitted several important new conclusions to be drawn. Thus the substance of this communication is based on the MCD information, 77°K electronic absorption spectra, crystal field calculations, and ir and laser Raman band locations in far-ir and lattice mode regions. Several X-ray parameters of a *trans*-$[Ni(py)_4I_2]$ crystal are also given.

There have also appeared a number of other interesting

(1) A. D. Buckingham and P. J. Stephens, *Annu. Rev. Phys. Chem.*, 17, 399 (1966).

(2) M. J. Harding, S. F. Mason, D. J. Robbins, and A. J. Thomson, *J. Chem. Soc. A*, 3047 (1971).

(3) M. J. Harding, S. F. Mason, D. J. Robbins, and A. J. Thomson, *J. Chem. Soc. A*, 3058 (1971).